Meso-tetrakis(*N*-methylpyridinium-4-yl)porphyrin at the Minor Groove of Contiguous Adenine-Thymine Base Pairs

Youn-Hee Chae, Biao Jin, Jong-Ki Kim,† Sung Wook Han,‡ Seog K. Kim, and Hyun Mee Lee*

Department of Chemistry, College of Sciences, Yeungnam University, Gyeongsan, Gyeongbuk 712-749, Korea
**E-mail: wbhyun@yumail.ac.kr*
†Department of Biomedical Engineering, School of Medicine, Catholic University of Daegu, Daegu 705-034, Korea
‡School of Herb Medicine Resource, Kyungwoon University, Gumi, Gyeongbuk 730-739, Korea
Received August 20, 2007

Three possible binding modes of cationic *meso*-tetrakis(*N*-methylpyridinium-4-yl)porphyrin (TMPyP) to d[(GCATATATGC)$_2$] duplex were investigated by the molecular dynamics (MD) simulation. Among the three binding modes namely, "along the groove", "across the groove" and "face on the groove", the "across the groove" model exhibited the largest negative binding free energy and the DNA backbone remained as the B form. In this model, the molecular plain of the TMPyP tilts 45° with respect to the DNA helix axis and is largely exposed to the solvent. TMPyP was stabilized mainly by the interaction between the positively charged neighboring pyridinium moieties of TMPyP and negatively charged phosphate groups of DNA. The result obtained in this work by MD and the report (Jin, B. *et al.*, *J. Am. Chem. Soc.* **2005**, *127*, 2417.) that the spectral properties of poly[d(A-T)$_2$] bound TMPyP in the presence and absence of the minor groove binding drug 4',6-diamidino-2-phenylindole are similar, we propose that TMPyP bind across the minor groove of the AT rich-DNA.

Key Words : *Meso*-tetrakis(*N*-methylpyridinium-4-yl)porphyrin, DNA, Minor groove, Molecular dynamics

Introduction

Over the past three decades, the interactions of DNA with various cationic porphyrins have been extensively studied not only for their potential application to photodynamic therapy but also as a probe for the DNA structure. *Meso*-tetrakis(*N*-methylpyridinium-4-yl)porphyrin (referred to as TMPyP) is one of the well known representatives of the porphyrin family. Various binding modes of TMPyP to DNA and synthetic polynucleotides, that depend on the [porphyrin]/[DNA] ratio, salt concentration, and the nature of DNA sequence have been introduced. At a low [porphyrin]/[DNA] ratio, and low NaCl concentrations, TMPyP prefers to intercalate between GC base pairs[1-4] while spectroscopic studies suggested they bind at or near the minor groove of continuous AT sequences.[5-12] For instance, the spectral properties of TMPyP that bound to duplex poly(dA)·poly(dT) and the triplex poly(dA)·[poly(dT)]$_2$ were identical, indicating the location of TMPyP in the duplex is near the minor groove.[11,12] The side of TMPyP possesses a common structural motif with minor groove binding drugs such as crescent shapes that match the turn of the helical motif in DNA, positive charges, and a certain degree of rotational freedom. Therefore, it is possible that the side of TMPyP fits into the narrow minor groove and binds along the groove. However, it is equally possible that TMPyP binds across the groove and is stabilized by electrostatic interaction between positively charged pyridinium moieties and negatively charged phosphate groups. The spectral properties of TMPyP bound to AT polynucleotide have been reported similar in the presence and absence of the minor groove binding drug, 4',6-diamidino-2-phenylindole (DAPI), supporting the suggestion that TMPyP binds across the minor groove.[10] On the other hand, a few computation studies supporting that TMPyP binds along the groove have been appeared.[13,14] As a recent instance, the minor groove binding model of Mn(IV)-TMPyP that binds along the groove with its side towards the helical axis has been reported.[13]

The experimental result that suggests the possibility of the binding of TMPyP across the minor groove motivated us to compare the stabilization energies obtained from molecular dynamic for the models that include the binding of TMPyP along the groove, across the groove and the facing the groove models.

Methods

Starting models. The structure of duplex starting model d[(GCATATATGC)$_2$] oligonucleotide for canonical B-DNA conformation was constructed using the program Hyperchem 7.0. The structure of TMPyP was obtained from the NMR structure by Phan *et al.* with the PDB ID code 2A5R[15] and X-ray crystallography.[16] The force field of TMPyP obtained from general AMBER force field (GAFF) parameter for small organic molecules to facilitate simulations of drugs and small molecule ligands in conjunction with biomolecules. The partial charges of TMPyP was calculated with the B3LYP/6-31G* basis set in the Gaussian98 program[17] and two stages of restrained electrostatic potential (RESP)[18,19] using the antechamber module in Amber 7.0.[20] The starting structures of the TMPyP-DNA complexes were built by considering experimental evidences that suggest that

TMPyP situated at the AT-rich DNA minor groove[5-12] and TMPyP binds across the minor groove of DNA.[10] The docking was induced from the three possible positions of TMPyP, namely "along" and "across" the minor groove and "face on" the minor groove. "Along" conformation denotes the binding of TMPyP at narrow and deep groove of DNA, and "across" presents the conformation in which the interaction of positively charged nitrogen at two neighboring pyrimidiumyl groups of TMPyP and negatively charged phosphate groups of DNA. The "face on" conformation indicates such a conformation in which nitrogen atoms at diagonal pyrimidiumyl groups of TMPyP contact with the phosphate groups of DNA (see result and discussion part).

The structures of the TMPyP-DNA complexes were constructed with the NMR structure of TMPyP and the nucleic acid in Hyperchem7.0 program.

Molecular dynamic simulation. The molecular dynamics (MD) simulation was performed using the AMBER 7.0 program. In order to neutralize the [d(GCATATATGC)$_2$]-TMPyP complex, Na^+ ions were added and solvated with explicit water molecules using the LEAP module of AMBER. The parm99.dat force field was used for this process. The sizes of the periodic boxes were ~53 Å × 60 Å × 60 Å, ~54 Å × 60 Å × 65 Å, and ~52 Å × 60 Å × 57 Å for the "along the groove", "across the groove", and "face on the groove" starting model, respectively. Long range electrostatic interaction which was calculated using Particle Mesh Ewald (PME)[21,22] was limited to 10 Å. Three steps were employed for the energy minimization. In the first step, the energy of the complex was minimized by 500 steps of the steepest descent method. Then 500 steps of the conjugate gradient method were performed for solvent and counter ions. During these two processes, both oligonucleotide and TMPyP were restrained at 500 kcal/mol·Å^{-2}. In the second step, calculations involve 2000 steps of steepest descent method and 2000 steps of the conjugate gradient method were performed without any restraint. Dynamic simulation with 2 fs increment for 5 ns was carried on in the final step. The oligonucleotide near the binding site of TMPyP was restrained by 50 kcal/mol·Å^{-2} to keep TMPyP at the oligonucleptide binding site during the simulation. More precisely, the number 6, 7, 16, and 17 bases in the "along the groove" model, 5, 7, 15, and 17 bases in the "across the groove" model and 6, 8, 16, 18 bases in the "face on the groove" model were restrained during the simulation. The SHAKE algorithm[23] was applied to constrain all bonds involving hydrogen atoms with a tolerance of 10^{-5} Å. The temperature was raised from 0 K to 300 K and the pressure was fixed at 1 atm.

Root mean-square deviations (rmsd) from the initial structures by the trajectories were calculated using the PTRAJ modules of AMBER 7.0. The average structures were obtained from the last 1ns simulation times. DNA conformations were analyzed by the CURVES program.[24] The final structure of the complexes was visualized by Visual Molecular Dynamics (VMD).[25] Computations were carried out IBM p690 system in the supercomputer center of the Korea Institute of Science and Technology Information (KISTI, Daejon, South Korea).

Free energy analyses. The energetic analysis was performed using the MM-GBSA module of the AMBER suite of program. MM-GBSA is able to calculate the relative stabilities of different conformations by dividing the total free energy into its single contributions. The free energies were estimated by averaging final structures with water molecules and counterions removed. The free energies for each porphyrin complex bound with the DNA duplex was computed with equation $G_{tot} = E_{gas} + G_{sol} - TAS$. The molecular mechanics of a molecule in the gas phase, E_{gas} is contains the contributions of the all internal energy (bonds, angles, dihedral angles) and non-bonded (van der Waals and electrostatic) interactions. The solvation free energy (G_{sol}) is estimated from the electrostatic solvation energy (G_{GB}) and the nonpolar solvation energy ($G_{nonpolar}$). The solute entropic contribution was investigated by normal mode analysis using NMODE module[26,27] in the AMBER package. The temperature was set to 300 K, consistent with MD simulations. The differences in the free energies were calculated by substracting the values of the free DNA and ligand from the complexes.

Results and Discussion

Optimized structures of the [d(GCATATATGC)$_2$]-TMPyP complex. The root-mean-squared deviation (RMSD) values are good indicators to justify if the system reached at the equilibrium. The progress of MD calculation results are examined by comparing the RMSD values of the 5 ns MD simulation for those of the corresponding initial structure as presented in Figure 1. This result reveals that all simulation system reach equilibrium within nanosecond scale. The averaged RMSD values of MD simulation are 3.49 Å, 1.97 Å, 1.47 Å, and 1.33 Å for DNA, "along the groove", "across the groove", and "face on the groove" model, respectively. The average RMSD values of the three TMPyP-DNA com-

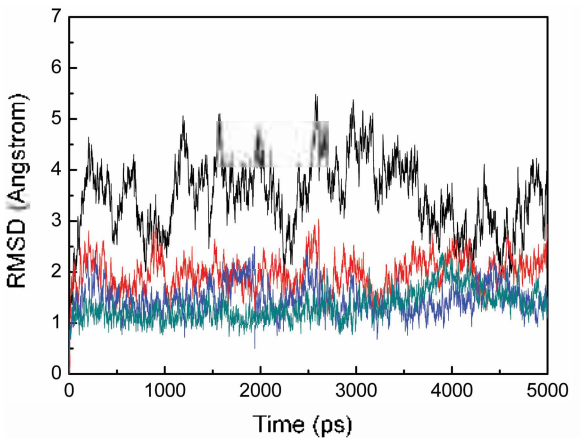

Figure 1. Root-mean square deviations (RMSD) for the TMPyP-free [d(GCATATATGC)$_2$] (black), and that of the along the groove (red), across the groove (blue), and face on the groove (green) models.

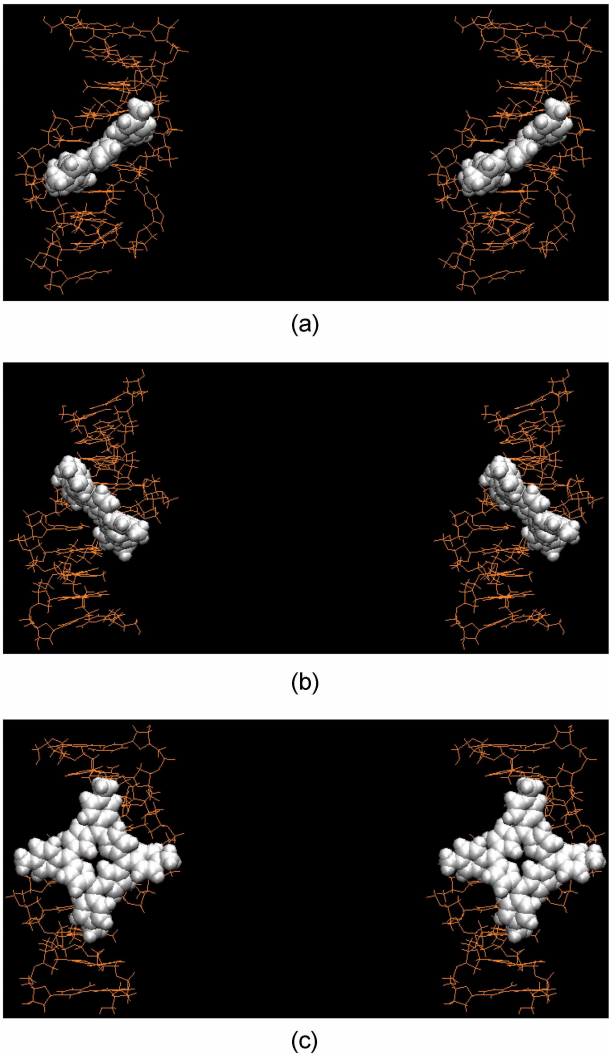

Figure 2. Representations of the [d(GCATATATGC)$_2$]-TMPyP complex. DNA is shown in orange and TMPyP white. (a) The crescent shape of side of the TMPyP molecule fit deep along the minor groove and is stabilized by hydrophobic interaction; (b) TMPyP binds across the minor groove and is stabilized by electrostatic interaction with phosphate group; (c) The molecular plane of TMPyP facing on the DNA bases and is stabilized by electrostatic interaction.

plexes are lower than TMPyP-free oligonucleotide, because the latter was simulated in a less constrained condition.

The stereoview of the resulting models from molecular dynamic method are depicted in the Figure 2. In the model shown in the Figure 2(a), which is assigned to "along the groove" model, two pyridinium moieties of TMPyP are inserted in the minor groove and other two are exposed to the solvent. It is note worthy that the hydrogen bonds between guanine and cytosine base pair between the 11th and 12th cytosine, those are appeared at the bottom of the Figure 2(a), is broken. The guanine base at the 11th position swings out from inside the DNA helix and is located down the paper plane. Although the reason for the "swinging out" of the guanine base is not clear at this point, overall shape of the DNA for this binding model is largely departed from ordinary B form. In the "along the groove" model the crescent shape on the side of the TMPyP molecule matches the helical turn. This complex seems to be stabilized mainly by the hydrophobic effect. No evidence for the formation of hydrogen bond between any DNA moieties and TMPyP was found.

In the model shown in Figure 2(b), the positive charges of the pyridinium rings are in contact with negatively charged phosphate groups of A7 and A17 residues hence the main force to form a complex is electrostatic interactions. The shape of DNA in the presence of TMPyP remains as overall B form. TMPyP in the "across the groove" model exposures larger extent compared to that in the "along the groove" model. In "across the groove" model, the distance between the positive charges between pyridinium is 11.1 Å, which matches with that of negative charges of 11.9 Å between the DNA phosphate groups. In this model, the molecular plane of TMPyP distorted and the N atom at the pyrrole moieties poke up to the 5'G direction. Whether the all four pyridinium rings are in contact with phosphate groups or not, the dihedral angles of 40-45° between porphyrin plane and the pyridinium plane were found. Another type of possible electrostatic interaction is shown in Figure 2(c), in which the positive charges of pyridinium moieties at the opposite side of TMPyP, which are apart by 15.7 Å, interact with the phosphate groups of T18 and T8 whose distance is 13.9 Å. Other two positive charges of TMPyP locate near the T18 and T8. The distance between the TMPyP's positive charges and the phosphate groups of those two phosphate groups are about 5.0 Å-6.0 Å.

The binding free energy as a criterion of the stability. The gas-phase energies, solvation free energies, and entropies for the TMPyP, oligonucleotide, and the three complexes were calculated from the MD simulation using MM/GB-SA and normal-mode analysis and are summarized in Table 1. The binding free energy components of the various TMPyP-oligonucleotide complexes are given in Table 2. In the Table 3, the binding free energy is defined by the difference in free energy *i.e.*, the binding free energy obtained by the subtraction of the sum of free energy of DNA and

Table 1. The energy contribution of the DNA, TMPyP and various TMPyP-oligonucleotide complexes (kcal/mol)

	free DNA	free-TMPyP	along	across	face on
E_{int}	846.89	139.24	1040.41	984.01	975.98
E_{elec}	714.93	26.37	350.84	335.31	342.82
E_{vdw}	−312.53	−9.49	−358.58	−327.28	−333.62
E_{gas}	1249.29	349.71	1032.67	1012.04	985.19
G_{nonpol}	18.72	2.75	19.94	21.19	21.09
G_{GB}	−2230.85	−37.72	−1837.26	−1830.91	−1786.33
G_{sol}	−2212.12	−34.96	−1817.32	−1809.73	−1765.24
$G_{gas+solv}$	−962.83	314.75	−784.65	−797.69	−780.05
TS_{tot}[a]	462.49	67.94	510.26	504.00	515.81
G_{tot}	−1425.32	246.81	−1294.91	−1301.69	−1295.87

[a] T = 300 K

Table 2. Binding free energy components for the various TMPyP-oligonucleotide complexes (kcal/mol)

	along	across	face on
ΔE_{int}	−139.31	−195.71	−203.74
ΔE_{elec}	−390.46	−405.99	−398.48
ΔE_{vdw}	−36.56	−5.50	−11.60
ΔE_{gas}	−566.33	−607.20	−613.82
ΔG_{nonpol}	−1.53	−0.28	−0.38
ΔG_{GB}	431.31	437.66	482.24
ΔG_{solv}	429.76	437.38	481.86
$\Delta G_{gas-solv}$	−136.57	−169.82	−131.97
$T\Delta S_{tot}$[a]	−20.17	−26.43	−14.62
ΔG_{bind}	**−116.40**	**−143.39**	**−117.35**

[a]T = 300 K

TMPyP from that of the TMPyP-DNA complex. The binding free energy of the "across the groove" model is far negatively larger being −143.39 kcal/mol compared to those of the "along the groove" and the "face on" the groove models. The latter two complexes show similar −116.40 kcal/mol and −117.35 kcal/mol, respectively. The "across the groove" model is favorable than "along the groove" by 26.99 kcal/mol.

In addition, the binding free energy change $\Delta G_{gas+solv}$ was decomposed to components of contribution from the internal, van der Waals, coulomb and polar solvation, and nonpolar solvation free energy. $\Delta G_{gas+solv}$ for "across" model is most stable among the three complexes tested in this work.

The difference in the binding energy between the models denoted by "along" and "across the groove" (Figures 2(a) and (b)) can be explained by the nature of the interaction. The former is stabilized by hydrophobic interaction while the latter by the electrostatic interaction. In comparison with other classical minor groove binding drugs such as DAPI for which the hydrophobic interaction is the major driving force to form a complex with DNA, TMPyP can not be inserted deep in the groove probably due to the steric hindrance of the pyridiniumyl ring. The two positive charges of TMPyP exposed to the solvent may also take a positive role for the stability. The binding energy of the "face on" model is far smaller compared to that of the "across" model in spite of the same origin of the interaction. The difference in the stability may be understood by the difference in the distance between the positive charges of TMPyP and the negative charges of the interacting phosphate groups of the oligonucleotide. In the "across the groove" model, the distance of the positive charges of TMPyP coincides with those between the phosphate groups of the B form DNA while it is not the case in the "face on" model.

The torsion angles of the AT oligomer and the stable "across" model are summarized in Table 3. The torsion angles, α, β, γ, ε, and ζ are closely similar and appeared to

Table 3. Torsion angles of the DNA and across model after molecular dynamics

complex		α	β	γ	δ	ε	ζ	χ
	strand 1							
	5'T	−77.5	166.1	51.9	106.3	188.6	−83.9	−131.3
	A	−77.4	170.3	66.4	108.5	198.3	−99.1	−125.6
	T	−62.7	185.5	66.1	116.6	164.1	−93.6	−100.6
	3'A	−53.7	177.6	52.9	129.8	184.9	−95.5	−136.7
DNA	strand 2							
	5'T	−62.6	166.8	59.4	118.1	187.1	−80.1	−133.6
	A	−74.8	162.6	55.8	82.5	189.8	−80.0	−155.8
	T	−67.1	187.8	76.0	119.2	199.9	−76.2	−134.8
	3'A	−139.4	197.8	30.6	118.4	179.2	−106.3	−87.9
	average	−76.9	176.8	57.4	112.4	186.5	−89.3	−125.8
	strand 1							
	5'T	−63.7	167.2	53.7	121.2	173.2	−85.9	−101.6
	A	−63.6	168.3	64.0	106.6	182.8	−78.3	−124.1
	T	−62.5	171.9	57.5	84.9	185.3	−84.1	−135.7
	3'A	−81.8	177.8	52.7	135.5	189.7	−91.4	−110.6
across	strand 2							
	5'T	−54.3	143.9	55.3	132.8	201.6	−102.5	−118.3
	A	−75.8	189.1	68.8	96.0	173.4	−67.6	−135.5
	T	−66.9	160.8	44.5	139.4	200.9	−148.9	−87.0
	3'A	−61.8	179.5	56.3	141.0	181.3	−87.8	−127.2
	average	−66.3	169.8	56.6	119.7	186.0	−93.3	−117.5
BDNA[a]		−61	180	57	122	−187	−91	−119

[a]Torsion angles from energy refined B-DNA[28]

be gauche+, trans, gauche-, in the order given for both compounds. Therefore, the backbone of DNAs, whether it is TMPyP-free or TMPyP bound across the minor groove, is essentially the same as that of energy-refined B-DNA,[28] indicating that the DNA in this complex maintain B form. While similar backbone angles were obtained for the "face on" the groove model (data not shown), the guanine base at the 11th position swings out from DNA helix in the "along the groove" model, deviating from the B form, as it was discussed in the previous section.

Comparing the reported binding modes with the result obtained in this work. The binding site of TMPyP to AT-rich DNA has been suggested to be the minor groove by circular and linear dichroism study.[11,12] The shape of the CD spectrum of TMPyP when bound to duplex $d(A)_{12}{\cdot}d(T)_{12}$ duplex at a low **[TMPyP]/[DNA]** ratio was similar to that bound to $d(A)_{12}{\cdot}[d(T)_{12}]_2$ triplex. Considering the major groove of DNA is blocked by the third $d(T)_{12}$ strand, TMPyP was suggested to locate at the minor groove. On the other hand, there have been at least two reports that support the major groove binding of TMPyP by NMR,[29] and magnetic circular dichroism (MCD) and linear dichroism (LD)[30] study. A recent NMR and molecular modeling docking study[29] showed that a TMPyP molecule binds at the major groove. However, the ratio **[TMPyP]/[DNA]** in the NMR study was 0.5 and 1.0 and at these high **[TMPyP]/[DNA]** ratios, TMPyP has been known to stack in the major groove.[11,12] Hence, the model that the single TMPyP docking in the major groove may not properly explain the NMR result. Based on the facts that the MCD result[30] that showed a weak perturbation between porphyrin and the DNA bases and the angle of two transition moments of porphyrin with respect to the DNA helix axis of 41° and 48° from LD measurement,[5] and very small red-shift in electric absorption spectrum upon binding to DNA a major groove binding mode for porphyrin was suggested.[30] However, other binding mode such as "across the groove" binding mode will result in a similar weak perturbation in MCD. Furthermore, the reported angles of 41° and 48° of TMPyP's transition moments relative to the DNA helix axis are based on the assumption that the B_x and B_y transitions are degenerate. In the complex, the interactions of these two transition moments with DNA are different and as a result, the degeneracy should be partially removed. From the partial removing of the degeneration, the two angles were reported as 70-82° and 55° for both the TMPyP-poly(dA)·poly(dT) and -poly[d(A-T)$_2$] complex.[10] Considering all these experimental reports, the calculation was limited to the models in which TMPyP locates at the minor groove.

Regarding the minor groove binding of TMPyP, an experimental work reported that the spectral properties of TMPyP in the presence and the absence of a minor groove binding drug DAPI are the same.[10] Considering that DAPI binds deep in the minor groove,[31-35] this observation suggests that any part of TMPyP does not insert deep in the minor groove. Porphyrin binding "along" the minor groove in which crescent-shaped side fits in the DNA helix turn has been suggested from the computational work.[29,30] For instance, optimized structure of the oxyl-(hydroxo)-Mn(IV)-TMPyP binds along the minor groove with its side towards the helical axis. However, this model cannot explain the simultaneous binding of DAPI and TMPyP with their retained spectral properties upon binding to DNA.[10] Furthermore, there is no indication from both theoretical studies[29,30] that the energy of the "along" and the "across" the minor groove binding mode are directly compared. From the result obtained in this work by molecular dynamics and the reported various studies is similar, we propose that "across the groove" model.

Conclusion

Among the models shown in this work, possibility of the "face on" model can be easily rejected not only from the binding energy but also from the experimental work. As it was discussed above, both angles of the B_x and B_y transition relative to the DNA helix axis in this model is close to 45°, which does not agree with reported value of 70-82° and 55°.[10] The angles observed from both the "along the groove" and "across the groove" models seem to match reported values. However, (1) the fact that the binding energy of the "across the groove" model is far larger than "along the groove" model, (2) the B form of the oligonucleotide remains in the "across the groove" model, while the guanine base at the end loose its hydrogen bond and swings out the DNA helix in the "along the groove model", and (3) the spectral properties of TMPyP bound to poly[d(A-T)$_2$] resemble in the presence and the absence of DAPI[10] led us to conclude that TMPyP probably binds across the minor groove of DNA.

Acknowledgement. This work was supported by an internal research grant of Yeungnam University. Dr. Lee appreciates the support from Korea Research Foundation for Research Fellowship (KRF-2005-050-C00003).

References

1. Marzilli, L. G.; Banville, L. D.; Zon, G.; Wilson, W. D. *J. Am. Chem. Soc.* **1986**, *108*, 4188-4192.
2. Strickland, J. A.; Marzilli, L. G.; Wilson, W. D. *Biopolymers* **1990**, *29*, 1307-1323.
3. Guliaev, A. B.; Leontis, N. B. *Biochemistry* **1999**, *28*, 15425-15437.
4. Lee, Y.-A.; Lee, S.; Cho, T.-S.; Kim, C.; Han, S. W.; Kim, S. K. *J. Phys. Chem. B* **2002**, *106*, 11351-11355.
5. Sehlstedt, U.; Kim, S. K.; Carter, P.; Goodisman, J.; Vollano, J. K.; Nordén, B.; Dabrowiak, J. C. *Biochemistry* **1994**, *33*, 417-426.
6. Schneider, H. J.; Wang, M. *J. Org. Chem.* **1994**, *59*, 7473-7478.
7. Yun, B. H.; Jeon, S. H.; Cho, T.-S.; Yi, Y.; Sehlstedt, U.; Kim, S. K. *Biophys. Chem.* **1998**, *70*, 1-10.
8. Lee, S.; Heon, S. H.; Kim, B. J.; Han, S. W.; Jang, H. G.; Kim, S. K. *Biophys. Chem.* **2001**, *92*, 35-45.
9. Lee, S.; Lee, Y.-A.; Lee, H. M.; Lee, J. Y.; Kim, D. H.; Kim, S. K. *Biophys. J.* **2002**, *83*, 371-381.
10. Jin, B.; Lee, H. M.; Lee, Y.-A.; Ko, J. H.; Kim, C.; Kim, S. K. *J. Am. Chem. Soc.* **2005**, *127*, 2417-2424.
11. Lee, Y.-A.; Kim, J.-O.; Cho, T.-S.; Song, R.; Kim, S. K. *J. Am.*

Chem. Soc. **2003**, *125*, 8106-8107.
12. Kim, J.-O.; Lee, Y.-A.; Yun, B. H.; Han, S. W.; Kwag, S. T.; Kim, S. K. *Biophys. J.* **2004**, *86*, 1012-1017.
13. Arnaud, P.; Zakrzewska, K.; Meunier, B. *J. Comput. Chem.* **2003**, *24*, 797-805.
14. Ford, K. G.; Pearl, L. H.; Neidle, S. *Nucleic Acids Res.* **1987**, *15*, 6553-6562.
15. Phan, A. T.; Kuryavyi, V.; Gaw, H. Y.; Patel, D. J. *Nat. Chem. Biol.* **2005**, *1*, 167-173.
16. Hui, X.; Gresh, N.; Pullman, B. *Nucleic Acids Res.* **1990**, *18*, 1109-1114.
17. Frich, M. J.; Trucks, G. W.; Schlegel, H. B.; Scuseria, G. E.; Robb, M. A.; Cheeseman, J. R.; Zakzewski, V. G.; Montgomery, Jr. J. A.; Stratman, R. E.; Burant, J. C.; Dapprich, S.; Millam, J. M.; Daniels, A. D.; Kudin, K. N.; Strain, M. C.; Farkas, O.; Tomasi, J.; Barone, V.; Cossi, M.; Cammi, R.; Mennucci, B.; Pomelli, C.; Adamo, C.; Clifford, S.; Ochterski, J.; Petersson, G. A.; Ayala, P. Y.; Morokuma, Q.; Cui, K.; Malick, D. K.; Rabuck, A. D.; Raghavachari, K.; Foresman, J. B.; Cioslowski, J.; Stefanov, J. V.; Ortiz, B. B.; Liashenko, G.; Liu, A.; Piskorz, P.; Komaromi, I.; Gomperts, R.; Martin, R. L.; Fox, D. J.; Keith, T.; Al-Laham, M. A.; Peng, C. Y.; Nanayakkara, A.; Gonzalez, C.; Challacombe, M.; Gill, P. M. W.; Johnson, B.; Chen, M. W.; Wong, J. L.; Andres, W.; Head-Gordon, M.; Replogle, E. S.; Pople, J. A. *Gaussian 98*, Revision A. 3.; Gaussian, Inc.: Pittsburgh, PA, 1998.
18. Bayly, C. I.; Cieplak, P.; Cornell, W. D.; Kollman, P. A. *J. Phys. Chem.* **1993**, *97*, 10269-10280.
19. Cieplak, P. I.; Cornell, W. D.; Bayly, C.; Kollman, P. A. *J. Comput. Chem.* **1995**, *16*, 1357-1377.
20. Case, D. A.; Pearlman, D. A.; Caldwell, J. W.; Cheatham, T. E. III.; Wang, J.; Ross, W. S.; Simmering, C. L.; Darden, T. A.; Merz, K. M.; Stanton, R. V.; Cheng, A. L.; Vincent, J. J.; Crowley, M.; Tsui, V.; Gohlke, H.; Radmer, R. J.; Duan, Y.; Pitera, J.; Massova, I.; Seibel, G. L.; Singh, U. C.; Weiner, P. K.; Kollman, P. A. *AMBER7*; University of California: San Francisco, 2002.
21. Essmann, U.; Perera, L.; Berkowitz, M. L.; Darden, T.; Lee, H.; Pedersen, L. G. *J. Chem. Phys.* **1995**, *103*, 8577-8593.
22. Darden, T.; York, D.; Pedersen, L. G. *J. Chem. Phys.* **1993**, *98*, 10089-10092.
23. Ryckaert, J. P.; Ciccotti, G.; Berendsen, H. J. C. *J. Comput. Phys.* **1977**, *23*, 327-341.
24. Laver, R.; Sklenar, H. *CURVES 5.3*; Laboratorie de Biochimie Theorique CNRS, Institu de Biologie Physico-Chimique: Paris, France, 1990.
25. Humphrey, W.; Dalke, A.; Shulten, K. *J. Mol. Graphics* **1996**, *14*, 33-38.
26. Srinivasan, J.; Cheatham, T. E.; Cieplak, P.; Kollman, P. A.; Case, D. A. *J. Am. Chem. Soc.* **1998**, *120*, 9401-9409.
27. Kollman, P. A.; Massova, I.; Reyes, C.; Kuhn, B.; Huo, S.; Chong, L.; Lee, M.; Lee, T.; Duan, Y.; Wang, W.; Donini, O.; Cieplak, P.; Srinivasan, J.; Case, D. A.; Cheatham, T. E. *Acc. Chem. Res.* **2000**, *33*, 889-897.
28. Levitt, M. *Proc. Nat. Acad. Sci. USA.* **1978**, *75*, 640-644.
29. Ohyama, T.; Mara, H.; Yamamoto, Y. *Biophys. Chem.* **2005**, *113*, 53-59.
30. Arnaud, P.; Zakrzewska, K.; Meunier, B. *J. Comput. Chem.* **2003**, *24*, 797-805.
31. Larsen, T. A.; Goodsell, D. S.; Cascio, D.; Grzeskowiak, K.; Dikerson, R. E. *J. Biomol. Struct. Dyn.* **1989**, *7*, 477-491.
32. Mohan, S.; yathindra, N. *J. Biomol. Struct. Dyn.* **1991**, *9*, 695-704.
33. Eriksson, S.; Kim, S. K.; Kubista, M.; Nordén, B. *Biochemistry* **1993**, *32*, 2987-2998.
34. Kim, H.-K.; Kim, J. M.; Kim, S. K.; Rodger, A.; Nordén, B. *Biochemistry* **1996**, *35*, 1187-1194.
35. Vlieghe, D.; Sponer, J.; Van meervelt, L. *Biochemistry* **1999**, *38*, 16443-16451.